Letter

Toward Plasmonic Solar Cells: Protection of Silver Nanoparticles via Atomic Layer Deposition of TiO

Stacey D. Standridge, George C. Schatz, and Joseph T. Hupp

Langmuir, **2009**, 25 (5), 2596-2600• DOI: 10.1021/la900113e • Publication Date (Web): 05 February 2009

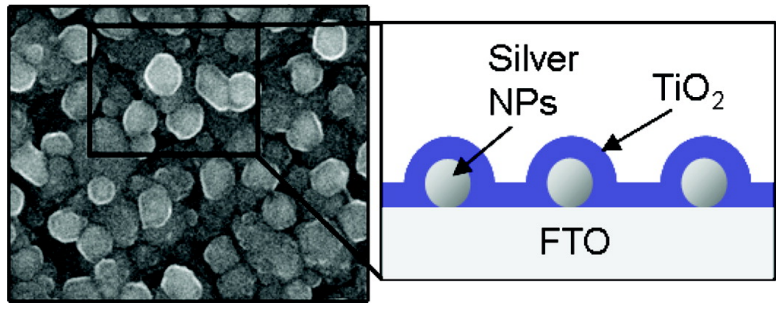

More About This Article

Additional resources and features associated with this article are available within the HTML version:

- Supporting Information
- Access to high resolution figures
- Links to articles and content related to this article
- Copyright permission to reproduce figures and/or text from this article

View the Full Text HTML

Toward Plasmonic Solar Cells: Protection of Silver Nanoparticles via Atomic Layer Deposition of TiO_2

Stacey D. Standridge, George C. Schatz, and Joseph T. Hupp*

Department of Chemistry, Northwestern University, 2145 Sheridan Road, Evanston, Illinois 60208

Received January 10, 2009

Plasmonic silver nanoparticles have unique properties that lend themselves to unusual optical applications, potentially including use as absorption amplifiers in dye-sensitized solar cells (DSSCs). However, these particles are easily damaged under oxidizing conditions. Atomic layer deposition of TiO_2 onto transparent-conductive-oxide-supported silver particles was examined as a means of protecting particles while simultaneously incorporating them into DSSC-functional photoelectrodes. The resulting assemblies were exposed to corrosive I^-/I_3^- solutions, and the degree of silver etching was determined via scanning electron microscopy and ultraviolet−visible spectroscopy. To form a pinhole-free (i.e., fully protective) crystalline TiO_2 layer, 7.7 nm (300 cycles) must be deposited. If, however, a 0.2 nm (2 cycles) Al_2O_3 adhesion layer is included, only 5.8 nm (211 cycles) of TiO_2 are necessary for the formation of a pinhole-free coating.

Introduction

Dye-sensitized solar cells (DSSCs) comprise a promising and potentially low-cost technology for light-to-electrical energy conversion. The cells generally employ high-area, mesoporous photoelectrodes consisting of a transparent semiconducting material (typically TiO_2), sensitized with an adsorbed molecular dye.[1,2] In this configuration, photoexcited dye molecules inject electrons into the porous semiconductor network, through which they diffuse until they are collected at the anode. The most efficient DSSCs employ I^-/I_3^- as the redox shuttle. They exhibit power conversions of 11%, roughly a third of the theoretical maximum for a cell of this design.[4] While there is room for improvement in cell photocurrent as well as fill factor, the parameter presenting the most room for improvement is the photovoltage. From the diode equation, it is clear that improvements in photovoltage can be achieved by decreasing the cell dark current,[4] which, in turn, can be accomplished by decreasing the photoelectrode surface area.

The functional challenge presented in reducing the photoelectrode surface area is to retain good light-harvesting efficiencies and, therefore, high photocurrents. One approach is to develop dyes presenting larger absorption cross sections.[5,6] A complementary approach is to couple dyes to plasmonic gold or silver nanoparticles (NPs).[7−9] The enhanced electromagnetic field near the particle is capable of greatly increasing the effective molecular (dye) absorptivity.[10] However, I^-/I_3^- is extremely corrosive toward silver and gold NPs. Care must be taken when designing plasmonic DSSCs to protect the plasmonic particles. At the same time, electromagnetic coupling between the NPs and the dye must be maintained. In this study, we examine the viability of titanium dioxide—the archetypal DSSC photoelectrode material—as an ultrathin barrier material for protection of plasmonic silver NPs against corrosion by I^-/I_3^- solutions. As a TiO_2 fabrication methodology, we have employed atomic layer deposition (ALD). We find that, in the absence of an adhesion layer, a pinhole-free barrier is formed after deposition of 7.7 nm (300 ALD cycles) of TiO_2. The inclusion of 0.2 nm (2 ALD cycles) of an Al_2O_3 adhesion layer reduces the thickness of TiO_2 required to form a pinhole-free barrier to 5.8 nm (211 ALD cycles).

Metallic NPs, usually silver or gold, interact with visible light to create a collective oscillation of the conduction electrons called a plasmon.[11] This phenomenon gives rise to two characteristic properties: an intense absorption feature at wavelengths resonant with the electron oscillation, and a greatly enhanced electromagnetic field near the particle. Notably, the maximum absorption wavelength of plasmonic particles has been found to be greatly dependent on factors such as size, shape, and dielectric environment.[11] These properties have been exploited in a variety of plasmonic applications ranging from sensing to enhanced fluorescence.[10,12−14] However, only a small number of studies have been performed on plasmonic DSSCs.[7−9] In typical experiments, the plasmonic particles were in direct contact with both the dye molecules and a Co(1,10-phenanthoroline)$_3^{2+/3+}$-based redox shuttle. The authors reported a small enhancement in the photocurrent red of the plasmon peak.[9] In contrast, unpublished experiments in our laboratory have shown that a similar redox shuttle (Co(4,4′-di-*tert*-butyl-2,2′-dipyridyl)$_3^{2+/3+}$) readily etches unprotected silver NPs. These results emphasize

* Corresponding author. E-mail: j-hupp@northwestern.edu.

(1) O'Regan, B.; Gratzel, M. *Nature* **1991**, *353*, 737–740.
(2) Martinson, A. B. F.; Hamann, T. W.; Pellin, M. J.; Hupp, J. T. *Chem.—Eur. J.* **2008**, *14*, 4458–4467.
(3) Nazeeruddin, M. K.; DeAngelis, F.; Fantacci, S.; Selloni, A.; Viscardi, G.; Liska, P.; Ito, S.; Takeru, B.; Gratzel, M. *J. Am. Chem. Soc.* **2005**, *127*, 16835–16847.
(4) Nelson, J. *The Physics of Solar Cells*; Imperial College Press: London, 2003.
(5) Youm, K.-T.; Nguyen, S. T.; Hupp, J. T. *Chem. Commun.* **2008**, 3375–3377.
(6) Hamann, T. W.; Jensen, R. A.; Martinson, A. B. F.; Van Ryswyk, H.; Hupp, J. T. *Energy Environ. Sci.* **2008**, *1*, 66–78.
(7) Zhao, G.; Kozuka, H.; Yoko, T. *Sol. Energy Mater. Sol. Cells* **1997**, *46*, 219–231.
(8) Wen, C.; Ishikawa, K.; Kishima, M.; Yamada, K. *Sol. Energy Mater. Sol. Cells* **2000**, *61*, 339–351.
(9) Ishikawa, K.; Wen, C.-J.; Yamada, K.; Okubo, T. *J. Chem. Eng. Jpn.* **2004**, *37*, 645–649.
(10) Pan, S.; Rothberg, L. J. *J. Am. Chem. Soc.* **2005**, *127*, 6087–6094.
(11) Kelly, K. L.; Coronado, E.; Zhao, L. L.; Schatz, G. C. *J. Phys. Chem. B* **2003**, *107*, 668–677.
(12) Aslan, K.; Wu, M.; Lakowicz, J. R.; Geddes, C. D. *J. Am. Chem. Soc.* **2007**, *129*, 1524–1525.
(13) Zhao, J.; Jensen, L.; Sung, J.; Zou, S.; Schatz, G. C.; VanDuyne, R. P. *J. Am. Chem. Soc.* **2007**, *129*, 7647–7656.
(14) Lakowicz, J. R.; Shen, Y.; D'Auria, S.; Malicka, J.; Fang, J.; Gryczynski, Z.; Gryczynski, I. *Anal. Biochem.* **2002**, *301*, 261–277.

10.1021/la900113e CCC: $40.75
Published on Web 02/05/2009

the need to physically isolate plasmonic NPs from the redox shuttle in DSSC applications.

ALD is a self-limiting process in which a binary series of volatile and highly reactive precursors are sequentially introduced into a sample chamber.[15] Each precursor forms on the substrate an intermediate monolayer with which the subsequent precursor reacts to form the product film. Purge periods between pulses are necessary to prevent chemical vapor deposition due to precursor intermixing. The wide variety of ALD precursors available allows for the deposition of a host of materials. Moreover, the mechanism of ALD elicits two key features: angstrom level control over the thickness of material deposited and the ability to coat high-aspect-ratio substrates conformally.[16] These features make ALD particularly well suited to DSSC photoelectrode fabrication.[17−23]

In this study, ALD was employed to coat silver NPs with varying thicknesses of TiO_2, and samples were exposed to a corrosive I^-/I_3^- solution. Pinholes in the TiO_2 allow I^-/I_3^- to come into direct contact with the NPs and etch them, eliminating the characteristic absorption feature. Conversely, a pinhole-free layer of TiO_2 isolates the NPs from I^-/I_3^-, preserving the particles. Thus, changes in the intense absorption of plasmonic NPs can be used to discern the presence of pinholes in TiO_2.

Experimental Methods

Silver Synthesis. Silver NPs were synthesized according to a literature procedure.[24] Briefly, silver oxide (0.3 g) was added to ultrapure water (300 mL). The mixture was heated to 70 °C and put under a hydrogen atmosphere. The reaction was allowed to proceed for 4 h.

Fluorine-doped tin oxide (FTO) was sonicated for 10 min each in soapy water, ethanol, and acetone. The slides were then soaked in a piranha solution (3:1 H_2SO_4:H_2O_2) for 30 min. An ethanolic solution of 4-(polyvinyl)pyridine (2 wt %) was used to functionalize the slides before they were heated for 1 h at 100 °C. Finally, the slides were soaked in the colloidal silver solution (NP diameter = 75 ± 5 nm) for 15 h.

ALD. A Cambridge Nanotech Savannah 100 ALD was used to deposit the desired thicknesses of TiO_2 and Al_2O_3 from titanium isopropoxide (TIP) and trimethyl aluminum (TMA) precursors. The chamber temperature was 200 °C, and the N_2 flow rate was 20 sccm. The TIP was held at 80 °C, and all other precursors were at room temperature. For the TiO_2 depositions, the TIP and water were each pulsed for 0.1 s. The TMA and water were each pulsed for 0.015 s for the Al_2O_3 depositions. The precursors were held in the deposition chamber for 1 s before a 12 s pump. Clean silicon chips were placed in the chamber with the samples. A J. A. Woolam Co. M2000 variable angle spectroscopic ellipsometer was used to analyze the ALD-coated silicon chips. TiO_2 thicknesses ranged from 3.6 to 9.5 nm (118 cycles to 344 cycles). The samples were annealed under N_2 for 30 min at 450 °C to attain oxide crystallinity. Sample configurations

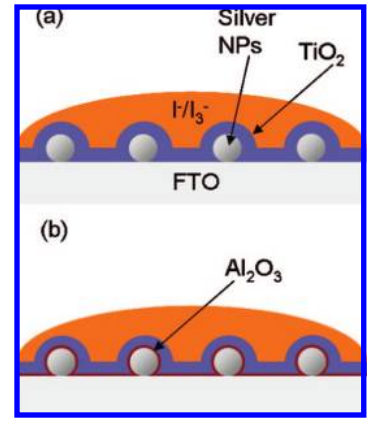

Figure 1. Sample configurations without (a) and with (b) a 0.2 nm (two cycles) Al_2O_3 adhesion layer.

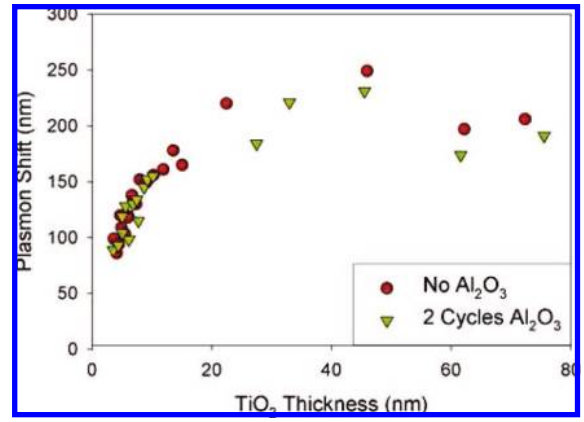

Figure 2. Shift of plasmon peak in the extinction spectra of silver NPs as a function of the thickness of TiO_2 deposited.

are shown in Figure 1 for samples with (Figure 1b) and without (Figure 1a) 0.2 nm (2 cycles) of an Al_2O_3 adhesion layer.

In view of the potential for poor growth of TiO_2 on silver, we reasoned that the metal-oxide thicknesses reported by silicon chips (standard ALD "control" substrates) might overestimate the thicknesses deposited on NPs. To assess this possibility, approximately 50 nm of silver was evaporated onto glass slides using an Edward Auto 306 E-Beam evaporator, and ALD runs of 109, 184, 259, and 333 cycles were performed concurrently on silicon and silver substrates. Ellipsometry was used to determine the thicknesses of TiO_2 deposited on each. Despite the fact that all of these cycles are greater than the ALD induction phase, we found that the growth rates differed from substrate to substrate. To account for this, we took the average of the growth rate differences at all four points. On the substrates with no adhesion layer, 1.14 times as much TiO_2 grew on silicon as on silver. In the presence of 0.2 nm (two cycles) of an Al_2O_3 adhesion layer, growth rates were more uniform, with about 1.07 times as much TiO_2 deposited on silicon versus silver. All thicknesses reported herein have been corrected for these differences.

Annealing Studies. Silver NP samples with 4.5 nm (129 cycles) of TiO_2 were annealed under N_2 in a ceramic tube furnace at 450 °C for 30 min. A high-area Whatman Anodisc (pore size = 200 nm) was coated with 20 nm (570 cycles) of TiO_2 and annealed at 450 °C in the tube furnace under N_2 for 30 min to 2 h. Powder X-ray diffraction (PXRD) patterns were recorded with a Rigaku XDS 2000 diffractometer using nickel-filtered Cu Kα radiation over a range of $10° < 2\theta < 50°$ in 0.1° steps with a 1 s counting time per step. Anodisc samples were placed in the diffractometer mounted on a stainless steel holder with double-sided tape. X-ray photoelectron spectroscopy (XPS) was performed on a silicon chip coated with 4.5 nm (129 cycles) TiO_2 using an Omicron ESCA probe with Al Kα

(15) Elam, J. W.; Groner, M. D.; George, S. M. *Rev. Sci. Instrum.* **2002**, *73*, 2981–2987.
(16) Elam, J. W.; Routkevitch, D.; Mardilovich, P. P.; George, S. M. *Chem. Mater.* **2003**, *15*, 3507–3517.
(17) Law, M.; Greene, L. E.; Radenovic, A.; Kuykendall, T.; Liphardt, J.; Yang, P. *J. Phys. Chem. B* **2006**, *110*, 22652–22663.
(18) Hamann, T. W.; Martinson, A. B. F.; Elam, J. W.; Pellin, M. J.; Hupp, J. T. *J. Phys. Chem. C* **2008**, *112*, 10303–10307.
(19) Hamann, T. W.; Martinson, A. B. F.; Elam, J. W.; Pellin, M. J.; Hupp, J. T. *Adv. Mater.* **2008**, *20*, 1560–1564.
(20) Elam, J. W.; Baker, D. A.; Martinson, A. B. F.; Pellin, M. J.; Hupp, J. T. *J. Phys. Chem. C* **2008**, *112*, 1938–1945.
(21) Elam, J. W.; Baker, D. A.; Hryn, A. J.; Martinson, A. B. F.; Pellin, M. J.; Hupp, J. T. *J. Vac. Sci. Technol., A* **2008**, *26*, 244–252.
(22) Martinson, A. B. F.; Elam, J. W.; Hupp, J. T.; Pellin, M. J. *Nano Lett.* **2007**, *7*, 2183–2187.
(23) Elam, J. W.; Martinson, A. B. F.; Pellin, M. J.; Hupp, J. T. *Chem. Mater.* **2006**, *18*, 3571–3578.
(24) Evanoff, D. D.; Chumanov, G. *J. Phys. Chem. B* **2004**, *108*, 13948–13956.

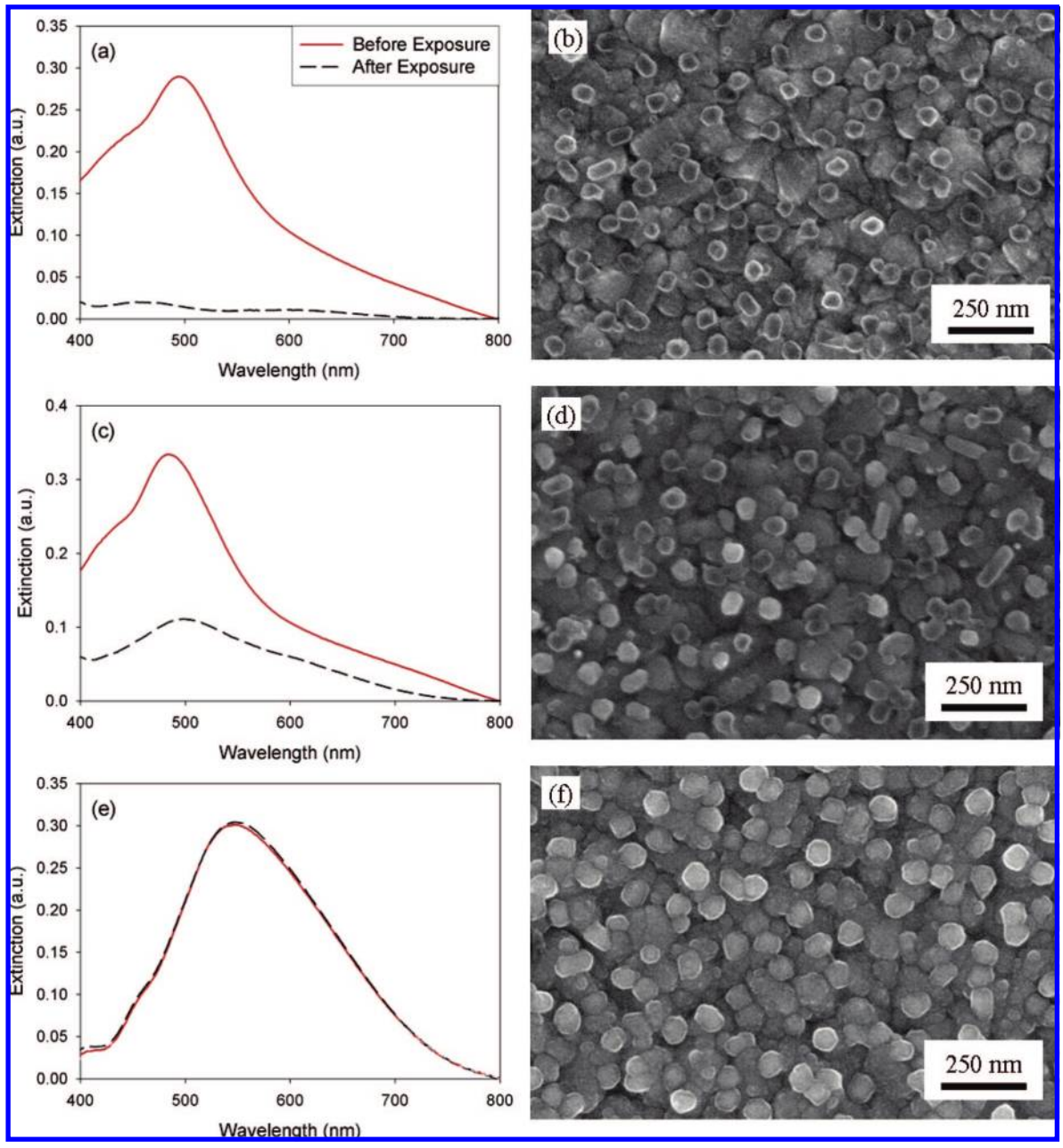

Figure 3. Characterization of samples after a 15 h of exposure to I^-/I_3^- in the dark. Data are representative of samples that were (a,b) completely etched, (c,d) partially etched, and (e,f) completely protected. (a,c,e) Extinction spectra before (solid line) and after (dashed line) exposure to I^-/I_3^-. (b,d,f) SEM micrographs of substrates after exposure to I^-/I_3^-.

radiation at an energy of 14 kV. Spectra were referenced to the C 1s peak at 284.7 eV.

Exposure to I^-/I_3^- A solution of 0.6 M LiI and 0.03 M I_2 in ethanol was prepared to give an I^-/I_3^- solution. This solution was dropcast on the samples, which were left covered for 15 h in the dark. Samples that showed little to no etching were then exposed to the same I^-/I_3^- solution under 1 sun illumination from a xenon light source with an AM 1.5 filter for 1 h. A Cary 5000 ultraviolet−visible−near-infrared (UV−vis−NIR) spectrometer was used to measure the visible extinction of the samples. Scanning electron microscopy (SEM) micrographs were taken on a Hitachi S-4800 SEM with a 10.0 kV accelerating voltage.

Results and Discussion

XPS and PXRD were used to characterize the TiO_2 after thermal annealing. The lack of a peak at 400 eV in the XPS spectrum (Figure S1) indicates that no nitrogen is incorporated during annealing. PXRD measurements revealed peaks at 25°, 38°, and 48° (Figure S2), characteristic of the anatase form (i.e., DSSC-relevant form) of TiO_2 (JCPDS card no: 21-1273). Visible-region electronic extinction spectra and SEM micrographs indicate that the silver NPs are preserved during annealing (data not shown).

Coating a plasmonic silver NP with TiO_2 red-shifts the absorbance of the particle as a result of the increase in the refractive index of the surrounding medium.[11] The extent of red-shifting depends on the thickness of the TiO_2. For TiO_2 thicknesses of less than 10 nm, the plasmon peak shifts linearly with thickness, implying a uniform rate of oxide deposition (Figure 2). Beyond a metal-oxide thickness of 10 nm, however, the plasmon shift begins to plateau. The thickness at which the

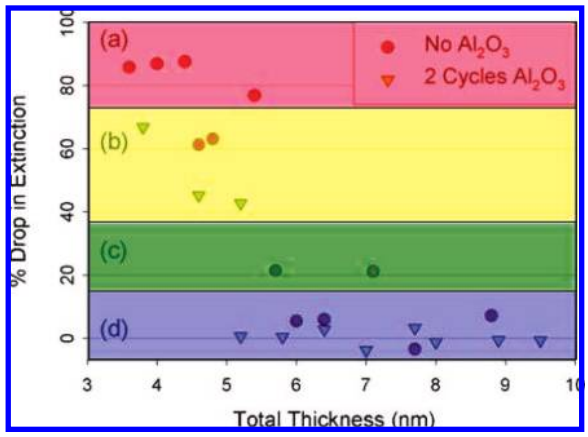

Figure 4. Percent drop in extinction of the silver NPs as a function of the total metal-oxide layer thickness. The degree of etching was determined by examination of SEM micrographs and UV−vis spectra. Samples were classified as (a) completely etched, (b) severely etched, (c) mildly etched, and (d) not etched.

shift plateaus is the "sensing distance" of the NP and is an approximate measure of the distance the enhanced electromagnetic field extends from the particle.[25] The comparatively small sensing distance observed here is likely a consequence of both the high refractive index of TiO_2 and the spherical shape of the silver particles.[26]

Representative extinction spectra and SEM micrographs are shown in Figure 3 for FTO samples featuring silver particles that were subsequently (i) completely etched (Figure 3a,b), (ii) partially corroded/etched (Figure 3c,d), or (iii) completely protected (Figure 3e,f) during exposure to I^-/I_3^-. Samples that were completely etched display extinction spectra similar to bare FTO. Revealingly, the micrographs show hollow shells—presumably TiO_2 that had formed on the NPs. Samples that were partially etched showed a drastic decrease in plasmon-based extinction, albeit not a complete elimination. Micrographs of these samples show a mix of hollow shells and unetched particles. No changes in extinction were discernible for samples that, by microscopy, appeared to have been completely protected from etching. Although TiO_2 can act as a photocatalyst under UV irradiation, the protected NPs remained stable with respect to irradiation over the course of several weeks, indicating that the NPs are not participating in any TiO_2-mediated reactions.

Figure 4 compares, for more than 20 samples, the percentage decrease in extinction of the silver NPs to the thickness of the metal-oxide barrier layer (see also Tables S1 and S2). Consistent with the examples in Figure 3, loss of plasmon extinction could be qualitatively correlated with the extent of etching as revealed by electron microscopy. Notably, samples featuring a thin Al_2O_3 adhesion layer consistently exhibited less etching for a given metal-oxide thickness. For samples lacking an Al_2O_3 adhesion layer, etching is significantly inhibited with 5.7 nm (200 cycles) of TiO_2 and completely inhibited with 7.7 nm (300 cycles). Samples featuring an adhesion layer display diminished etching with 5.0 nm TiO_2 coatings (177 cycles) and zero etching with 5.6 nm TiO_2 coatings (211 cycles) (i.e., total metal-oxide coating thicknesses of 5.2 and 5.8 nm). Thus the inclusion of an adhesion layer decreases the thickness required to form a fully effective barrier by ~2 nm.

Film growth by ALD depends exclusively on surface reactions. Thus, the substrate surface plays a crucial role in the ALD process. Hydroxylated surfaces are generally the most amenable to efficient ALD. Conversely, nonhydroxylated surfaces, such as silver, can present challenges. Accordingly, TIP does not react well with silver NPs. On the other hand, it has been demonstrated previously that TMA is able to deposit on a variety of "non-ideal" substrates, including synthetic polymers, cotton, and silver.[27−29] Al_2O_3 is an excellent adhesion layer because it can deposit on silver NPs and then present a hydroxylated layer for reaction with TIP.[30]

Finally, etching/stability studies were extended to conditions matching those in operating solar cells. Samples that were completely protected or only mildly etched were further exposed to I^-/I_3^- under 1 sun illumination for 60 min. Samples that were mildly etched in the dark were mildly etched in the light; samples that were unaffected in the dark remained unaffected under illumination.

As indicated above, our ultimate goal is to employ plasmonic NPs as amplifiers for dye-based light collection in photoelectrochemical solar cells. In this context, the alumina adhesion layer is advantageous because it enables corrosion protection to be achieved with a thinner TiO_2 layer, thereby allowing dye molecules to be placed closer to the plasmonic particles. While small in absolute terms, the 2 nm decrease in separation particle/dye separation distance afforded by inclusion of an alumina adhesion layer is significant in comparison to the 10 nm "sensing distance" noted above. More precisely, because the plasmon-enhanced electromagnetic field decays with the inverse cube of the distance from the center of the NP, the enhancement of molecular dye optical properties will be more pronounced closer to the metal particle.[11] On the other hand, the inclusion of an insulating Al_2O_3 layer in a solar cell could potentially inhibit current collection. Preliminary experiments indicate, however, that incorporation of 0.2 nm (2 cycles) of Al_2O_3 in plasmonic DSSCs does not diminish current collection.

Conclusion

In conclusion, we have prepared and exposed metal-oxide-coated silver NP films to an aggressive I^-/I_3^- environment (i.e., DSSC-like environment) to determine whether the oxides can protect the NPs from corrosion and photocorrosion. We find that 7.7 nm (300 cycles) of TiO_2 are required to form a fully protective barrier. However, inclusion of 0.2 nm (two cycles) of an Al_2O_3 adhesion layer reduces the required TiO_2 thickness to 5.8 nm (211 cycles). The use of an adhesion layer to reduce the minimum thickness of a pinhole-free TiO_2 layer may be beneficial in a host of applications, including plasmonic DSSCs and plasmon-based sensing in aggressive environments. Indeed, we intend to report on DSSC studies in the near future.

Acknowledgment. We thank Mary Faia and Chaiya Prasittichai for ellipsometry measurements and Karen Mulfort for obtaining X-ray data. We thank Prof. Michael Pellin and Dr. Jeff Elam for helpful discussions and for access to ellipsometry facilities at Argonne National Laboratory. SEM and XPS measurements were performed in the EPIC and

(25) Evanoff, D. D.; White, R. L.; Chumanov, G. *J. Phys. Chem. B* **2004**, *108*, 1522–1524.
(26) Haes, A. J.; Zou, S.; Schatz, G. C.; VanDuyne, R. P. *J. Phys. Chem. B* **2004**, *108*, 109–116.
(27) Groner, M. D.; Fabreguette, F. H.; Elam, J. W.; George, S. M. *Chem. Mater.* **2004**, *16*, 639–645.
(28) Hyde, G. K.; Park, K. J.; Stewart, S. M.; Hinestroza, J. P.; Parsons, G. N. *Langmuir* **2007**, *23*, 9844–9849.
(29) Whitney, A. V.; Elam, J. W.; Stair, P. C.; Van Duyne, R. P. *J. Phys. Chem. C* **2007**, *111*, 16827–16832.
(30) Kukli, K.; Ritala, M.; Leskelä, M.; Sundqvist, J.; Oberbeck, L.; Heitmann, J.; Schröder, U.; Aarik, J.; Aidla, A. *Thin Solid Films* **2007**, *515*, 6447–6451.

KECK-II facilities of the NUANCE Center at Northwestern University. The NUANCE Center is supported by NSF-NSEC, NSF-MRSEC, the Keck Foundation, the State of Illinois, and Northwestern University. We gratefully acknowledge financial support from the U.S. Department of Energy, Office of Science (Grant Nos. DE-FG87ER13808 and DE-FG02-03-ER15487).

Supporting Information Available: XPS spectrum of a Si chip coated with 4.5 nm TiO_2, PXRD patterns for commercial anodic aluminum oxide coated with 20 nm of TiO_2, and tables of ALD cycles, metal oxide thicknesses, and degree of etching. This material is available free of charge via the Internet at http://pubs.acs.org.

LA900113E